

An In-wheel Axial-flux-modulated Machine for Hybrid Electric Vehicles

S. L. Ho¹, Shuangxia Niu¹, W. N. Fu¹, and Jianguo Zhu²

¹Department of Electrical Engineering, The Hong Kong Polytechnic University, Kowloon, Hong Kong

²Faculty of Engineering, University of Technology, Sydney, P.O. Box 123, Broadway NSW 2007, Australia
eesxniu@polyu.edu.hk

Abstract —In this paper, a novel low-speed high-torque axial-flux-modulated permanent magnet motor (PM) is proposed for the gearless drive in hybrid electric vehicles (HEVs). It has a high torque density and power density, which enables it to be fitted inside the very limited space such as the wheel rim of HEVs. In the design, the key is that the proposed motor breaks the traditional rule which stipulates that the pole-pair numbers of the stator and the rotor must be equal and special iron segments are introduced in the airgaps to modulate the magnetic field based on the “magnetic gear” effect. Three-dimensional time stepping finite-element method is used to evaluate the transient and static performance of the proposed machine. With respect to the volume, efficiency, loss of the machines, the results are compared with those of a radial-flux-modulated motor with the same power output and rotation speed, using two-dimensional and three-dimensional finite-element methods.

I. INTRODUCTION

With an increasing concern on the environmental protection and energy conservation, there is an accelerating interest on the research of HEVs. Since the wheels of vehicles run in low speed and the dimension of electric machines is inversely proportional to its running speed, conventional direct drive electric motor is very bulk if the traction motor needs to produce a reasonable torque over a wide speed range. Normally, a mechanical gear is needed to reduce the motor speed. The use of a mechanical gear reduces the motor size, but increases the space to contain the gear. The mechanical gear also reduces the energy transmission efficiency. An energy-efficient and space saving motor driver is desirable for the development of HEVs. Benefiting from the absence of mechanical gears and independent control of wheels, direct-drive in-wheel electric motor driver needs a lower maintenance, and owns a saved space, an improved efficiency and the enhanced control flexibility and this technology is especially attractive for the electric propulsion systems in HEVs.

Recently, magnetic gears (MG) are proposed to compete with mechanical gears in terms of torque transmission capability and efficiency [1]. Compared to their mechanical counterparts, MGs have a highly competitive torque transmission capability with very high efficiency. The MG can be directly combined with a conventional permanent magnet (PM) motor inside one frame [2]. The system torque density can be significantly improved. However such system has two rotating parts and three airgaps. The mechanical structure is complex and the machine runs noisily.

A simple magnetic geared motor that integrates MG with a conventional outer-rotor PM brushless motor is presented recently [3]. According to the reported system, the MG is integrated with a conventional outer-rotor PM brushless

motor and there is only one rotary part. The outer-rotor is equipped with sintered NdFeB magnets. Fig. 1 shows such a motor. Its stator has a 3-phase concentrated winding which can produce a rotating magnetic field with 3 pole pairs, and the outer-rotor is equipped with 22 pole pairs. It has stationary iron segments which are made of silicon steel laminations to modulate the airgap field space harmonics, and the rotor can rotate at low speed. The operating principle of the setup is similar to that of MG. However, the high-speed rotary field is created by an armature rather than with magnets. The overall size of the unit is more compact than the motor and gear combination.

In this paper the idea of flux-modulation is creatively extended to double-rotor one-stator axial-flux PM motors, which have the advantage of compact structure and high efficiency. A novel low-speed axial-flux-modulated motor (AFMM) for the in-wheel gearless drive of HEV is proposed.

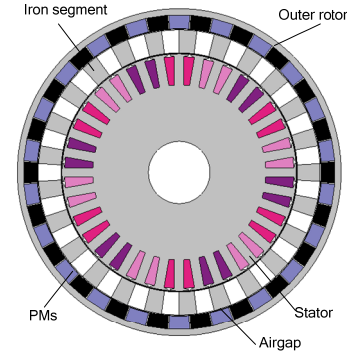


Fig. 1. An overview of an intersection structure of a radial-flux-modulated PM motor (Motor I).

II. PROPOSED AXIAL-FLUX-MODULATED MOTOR

The proposed AFMM has a 3-phase concentrated winding which can produce a rotary magnetic field with 3 pole pairs, and the outer-rotor has 22 pole pairs, as shown in Fig. 2. Iron segments in the airgap are used to modulate the magnetic field. It can operate with high power density at low speed, hence very suitable for the utilization in direct drives in HEVs. With AFMM, the front wheels and rear wheels can operate as a series-parallel drive without special mechanical coupling between them. The advantages of AFMM are summarized as:

(1) Due to the space constraints in the wheel, with the disc shape, this motor is well suited to direct couple with a wheel. Because the ratio between the airgap diameter and the axial length of iron cores is large, the axial-flux design can further boost the torque density significantly.

(2) The manufacture process of AFMM is much simpler than that of the radial-flux-modulated motor (RFMM). Both the iron segments and the stator are made

from soft magnetic compound (SMC) materials in modular structures and can be assembled easily [4].

(3) The coils on the two sides of the stator core are wound back-to-back toroidally in order to shorten the length of the end windings which share a common back iron, thereby saving the copper materials and improving the power density.

(4) The slot spaces can be efficiently used since it has small number of stator slots compared with those with conventional integral slot structure.

(5) The heat dissipation capability is good for the naturally formed ventilating ducts between the iron segments.

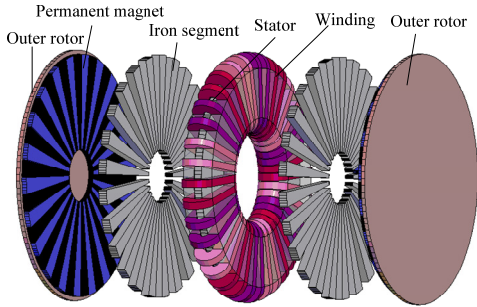


Fig. 2. Proposed axial-flux-modulated motor.

III. PERFORMANCE ANALYSIS AND COMPARISON

The design data are shown in Table I. The performances of AFMM are analyzed using 3-D time-stepping FEM [5]. The plot of magnetic flux density on the surface of rotor iron core is given in Fig. 3. It shows that at the rotor side, one can still see the three pole-pair magnetic field produced by the stator windings. The torque curve and back emf curves versus time at full-load are shown in Figs. 4 and 5, respectively. It is noted that the torque ripple is not very large and the three-phase back emf waveforms are symmetrical.

The performances of the two motors are summarized in Table II. The FEM simulations show that the AFMM produces about 40% higher torque when compared to that of RFMM. The coreloss of the AFMM is higher than that of the RFMM because the stator volume of the AFMM is smaller than that of the RFMM. However, because the AFMM has shorter end windings, the copper loss is small. Therefore, the total loss of the AFMM is smaller than that of the RFMM.

IV. REFERENCES

- [1] M. Aubertin, A. Tounzi and Y. Le Menach, "Study of an electromagnetic gearbox involving two permanent magnet synchronous machines using 3-D-FEM," *IEEE Trans. Magn.*, vol. 44, no. 11, Part 2, pp. 4381-4384, Nov. 2008.
- [2] K. T. Chau, Dong Zhang, J. Z. Jiang, Chunhua Liu and Yuejin Zhang, "Design of a magnetic-gear outer-rotor permanent-magnet brushless motor for electric vehicles," *IEEE Trans. Magn.*, vol. 43, no. 6, pp. 2504-2506, June 2007.
- [3] L. L. Wang, J. X. Shen, Y. Wang and K. Wang, "A novel magnetic-gear outer-rotor permanent-magnet brushless motor," *4th IET Conference on Power Electronics, Machines and Drives*, pp. 2-4 Apr. 2008, pp. 33-36.

- [4] M. A. Khan, P. Pillay, R. Guan, N. R. Batane, and D. J. Morrison, "Performance assessment of a PM wind generator with machined SMC cores," *IEEE International Electric Machines & Drives Conference*, vol. 2, 3-5 May 2007, pp. 1049-1053.
- [5] P. Zhou, W. N. Fu, D. Lin, S. Stanton and Z. J. Cendes, "Numerical modeling of magnetic devices," *IEEE Trans. Magn.*, vol. 40, no. 4, pp. 1803-1809, July 2004.

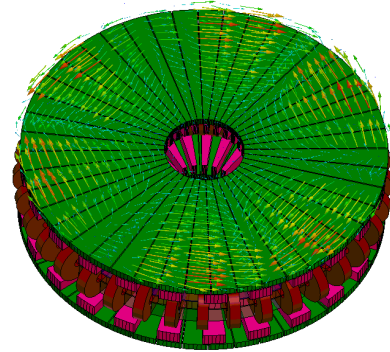


Fig. 3. The plot of magnetic flux density on the surface of rotor iron core (Motor II).

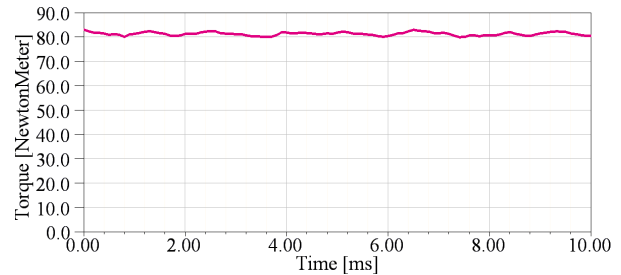


Fig. 4. The torque at full-load operation.

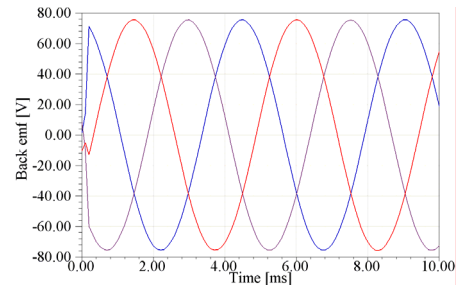


Fig. 5. The induced emf at full-load operation (Motor II).

TABLE I DESIGN DATA OF THE AXIAL FM MOTOR (MOTOR II)

Frequency	220 Hz
Total axial length	64 mm
Outside radius	92 mm
Inside radius	60 mm
Thickness of PM	3.9 mm
Thickness of stationary iron	6.5 mm
Number of outer rotor pole pairs	22
Number of stationary iron pieces	25
Number of stator pole pairs	3
Number of stator slots	36

TABLE II COMPARISON OF DIFFERENT MOTORS

Motor type	Motor I (Radial flux)	Motor II (Axial flux)
Output torque (Nm)	58.0	81.2
Coreloss (W)	59.0	98.5
Copper loss (W)	282.3	223.3
Total coreloss and copper loss (W)	341.3	321.8